ISBN: 978-3-95450-231-8 ISSN: 2673-5490 doi: 10.18429/JACoW-IPAC2023-THPA148

SLS 2.0 CROTCH ABSORBERS DESIGN

Colette Rosenberg, Jonas Buchmann, Karsten Dreyer, Nazareno Gaiffi, Romain Ganter, Björn Grossenbacher, Tino Höwler, Natalia Kirchgeorg, Lothar Schulz, David Stephan, Xinyu Wang, André Weber, Paul Scherrer Institut, 5232 Villigen PSI, Switzerland

Abstract

The installation of the new Swiss Light Source - SLS2.0 will start in October 2023. All beamlines will profit from the increased photon beam brightness. Given the geometrical constraints of the new storage ring, high synchrotron radiation power densities must be dissipated on the crotch absorbers. For the bending magnets, as well as the insertion devices, absorbers have been adapted to maximize their efficiency and protect downstream components. A design in Glidcop®, fitting a CF63 flange, has been developed to fulfill the space, vacuum and thermal requirements. This paper will describe the design, manufacturing and testing of first crotch absorbers of SLS 2.0.

SLS2.0 SPECIFICATION

Storage ring of SLS2.0 is based on a multibend achromat and antibend design with maximum electron energy of 2.7 GeV [1]. Given the tight space constraints of this lattice, the Synchrotron Radiation (SR) heat needs to be carefully dissipated to protect the vacuum components, seals and auxiliary equipment such as Beam Position Monitor (BPM) pickups. This will be executed through tapering surfaces of the vacuum chambers as well as SR Absorbers. They have been carefully studied and optimized to match the individual needs of SLS2.0 storage ring sections. Three main families can be distinguished (Fig. 1):

1) Closed Absorber that dissipates all the Synchrotron Radiation (SR) power generated by bending magnets where no light extraction is foreseen
2) First Crotch Absorber located near the bending magnets. It has a large window opening to pass maximal possible beam size while protecting downstream chamber. It dissipates most of the power.
3) Second Crotch Absorber located at the Front Ends entrance of the beamlines. They function is to precisely match the beam requirements of the beamlines, protect the optics components downstream and to dissipate the residual heat from the first absorber.

The undulator light goes through the windows of both absorber and is cut in special absorbers located in the front end. The goal for the vacuum system of SLS 2.0 Storage Ring is to reach an average pressure of 1.0×10^{-9} mbar (CO equivalent) with 100 mA.h of integrated beam current [2]. Seven discrete pumping units (with an Ion Getter and a NEG Pump) will be located along each of the twelve vacuum arc sectors. They will help to maintain the low pressure after the NEG coating inside the vacuum chambers is saturated. The Absorbers will be located inside those assemblies to minimize the effect of the high outgassing rates coming from their bodies, especially during the conditioning. Example of a crotch absorber integrated inside a pumping block is shown in Fig. 2.

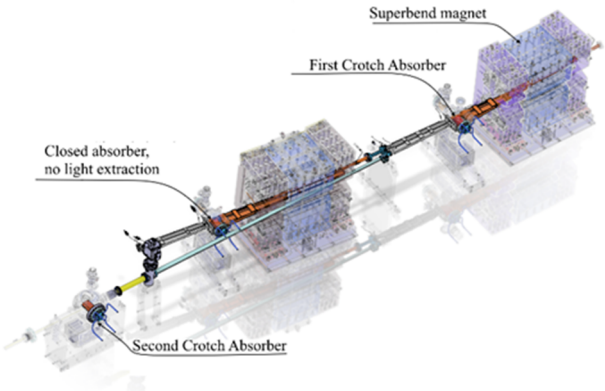

Figure 1: Arc with three absorbers.

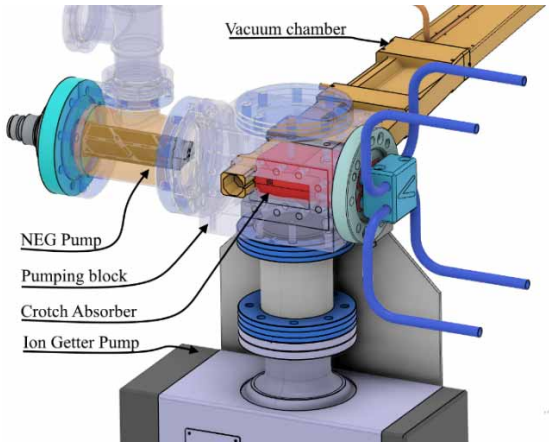

Figure 2: First Crotch Absorber inside a pumping block.

DESIGN PROCESS

Based on the magnetic field from the bending magnets, SYNRAD [3] and SPECTRA [4] simulations of the ring lattice were perform do define the heat load distribution. Maximal power was found to be at the level of 3.7 kW and 7.1 kW for the normal and super bend magnets, respectively. Example of the results are shown in Fig. 3. The following design criteria were applied in the process:

- Maximum 10 W/mm^2 power density on the water-cooled walls of the vacuum chambers
- Maximum 50 W/mm^2 and 400 °C on the absorber body if made out of glidcop (250 °C in case of CuCrZr).
- No Power dissipated in the gaskets and on flanges
- Maximum cooling water temperature lower than cooling water boiling point

ISBN: 978-3-95450-231-8 ISSN: 2673-5490 doi: 10.18429/JACoW-IPAC2023-THPA148

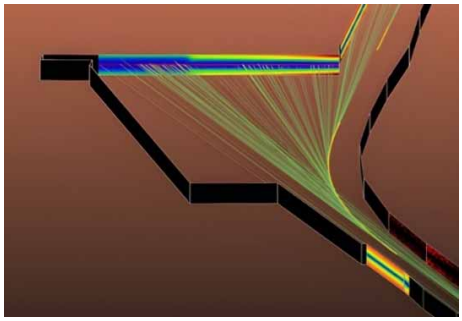

Figure 3: Synrad simulation of normal incidence for a 5T superbend magnet.

The existing SLS1 absorber design was considered but this geometry was not meeting the abovementioned criteria. Main optimizations included adding a second toothed jaw with a smaller opening angle. Additionally, it was decided to add a second absorber a few meters downstream which can be transversally moved for fine adjustment of pointing direction if needed.

Figure 4 shows an initial SYNRAD simulation of a first absorber for the 5T superconducting magnet. To sufficiently spread the SR power, an opening angle of only 2 degrees is used (1 degree per jaw). As a consequence, the electron beam orbit offset will have to remain within +/- 250 µm vertically. Total SR absorbed power was calculated to be 5.9 kW (rest of the initial 7.1 kW was sent further downstream to the second absorber), with a maximum heat load of 17 W/mm^2. These parameters were used as input for the Finite Element Modelling (FEM).

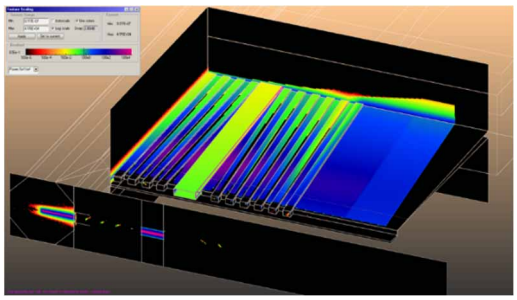

Figure 4: SYNRAD simulation of the 5T Superbend absorber.

FINITE ELEMENT MODELLING

Two absorber types were initially designed for different power dissipation: a normal bend absorber in the downstream of bending magnets for the power deposition up to 3.5 kW and a super bend absorber in the downstream of superconducting magnet for power absorption up to 6 kW. For energy up to 3.5 kW, the age-hardenable CuCrZr alloys was considered to meet the design requirements. High material hardness of CuCrZr enables the integration of Conflat type knife edge which reduces material and fabrication costs [5-7]. Dispersion strengthened Glidcop® AL-15 alloy was considered for super bend absorber given its high resistance to thermal stress.

The final model of absorber consisted of two Glidcop® water-cooled jaws fixed in a stainless-steel flange. Each jaw had a number of flat teeth and intermediate grooves, with the wedge of upper jaw loosely fitting into the grove of lower jaw, without any contact, even when there is thermal expansion due to synchrotron radiation. Each jaw had three holes of 10 mm ID for concentric cooling channels. The water velocity was 1.5 m/s. In the thermal calculation the heat transfer film coefficient was 15 kW/m^{2}K and water inlet temperature was 25 °C.

Power density distributions on absorber surfaces calculated from SYNRAD simulation were transferred into finite element (FE) model in ANSYS Workbench. In thermal mechanical calculations, spatial heat power density distribution was defined as TABLE using APDL command *DIM for each absorber beam intercepting surface. Due to the large number of faces, the repetitive APDL script generation was performed using a MATLAB program, which also converted the SYNRAD output data into the desired format for the ANSYS software. This approach enabled fast and efficient data transfer from SYNRAD to ANSYS.

To minimize the error in heat load mapping, a mesh seed size of 0.2 mm was selected, which was smaller than the SYNRAD mesh size on surfaces with high power density. For the remaining irradiated surfaces, the mesh seed size was 0.8 mm, while the general mesh size of the model was 2 mm. The finite element model consisted of a total of 3 million nodes and 2 million elements, presented in Fig. 5.

In the finite element analysis, stress, thermal deformation and temperature of absorber were calculated and verified against design criteria. The maximal temperature on absorber surface was 297°C (shown in Fig. 6) and maximal thermal stress was 171 N/mm^2. The maximal cooling water temperature was limited to 160°C, below the water boiling temperature at 6 bar.

Figure 5: Finite element model.

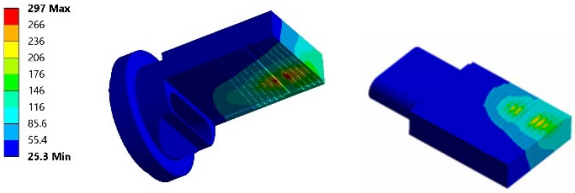

Figure 6: Results of FEA. Temperature in °C, power dissipation 5.9 kW.

A conjugate heat transfer (CHT) simulation was performed on a segment of an absorber body, which included a stainless steel water pipe and cooling water [8]. The absorber and cooling water temperatures were calculated using a direct coupling of ANSYS Thermal and Computational Fluid Dynamics (CFD) software ANSYS Fluent.

ISBN: 978-3-95450-231-8 ISSN: 2673-5490 doi: 10.18429/JACoW-IPAC2023-THPA148

The cooling water temperature and the convective heat transfer coefficient of the FE modeling were confirmed.

PROTOTYPE TESTING

A water-cooled absorber, made of CuCrZr, was tested in an e-beam welding chamber as shown in Fig. 7. The e-beam spot size was 10 mm, and the incident e-beam power was 3960 W, corresponding to an absorbed power of 3 kW on half of the absorber. The inlet and outlet water temperatures and temperatures on the absorber body were measured at different flow rates.

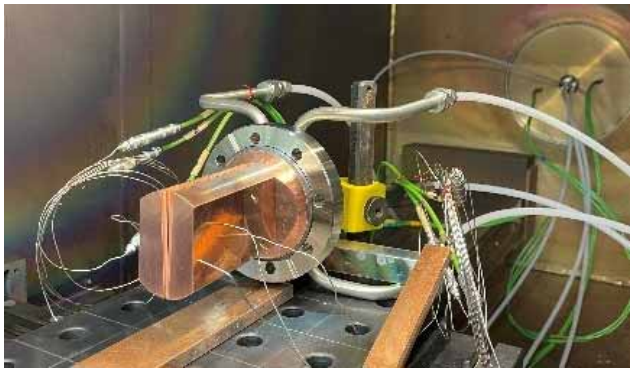

Figure 7: Prototype tested in e-beam welding chamber.

Results were compared with the simulations and showed a very high correlation. Cooling water temperature rose by 20 °C with a flow rate of 4.1 l/min when it flowed to both cooling circuits of absorber and resulting in a water velocity of 1.3 m/s. Maximal measured temperature of the absorber body was 70 °C.

Given the small opening angle, the correct alignment of the absorber during the assembly phase is essential for the machine operation. In Fig. 8 initial test of the prototype alignment inside of a pumping block is presented

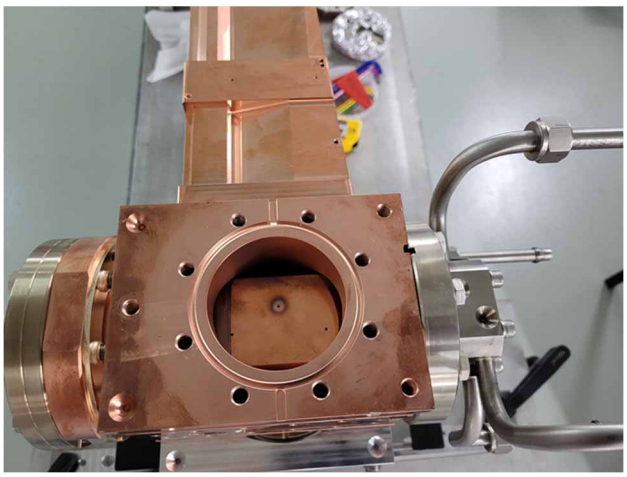

Figure 8: Alignment test of the absorber prototype.

MANUFACTURING ASPECTS

After the successful test of the prototype, the procurement process for the manufacturing of over 100 pieces has started. Since the cost of the CuCrZr and Glidcop absorber version were comparable, it was decided to choose Glidcop for all absorbers. Glidcop® can withstand higher temperature and was mandatory for the Superbend absorbers. All of them consist of the same number of elements, as shown in Fig. 9 (courtesy of FMB GmbH [9]).

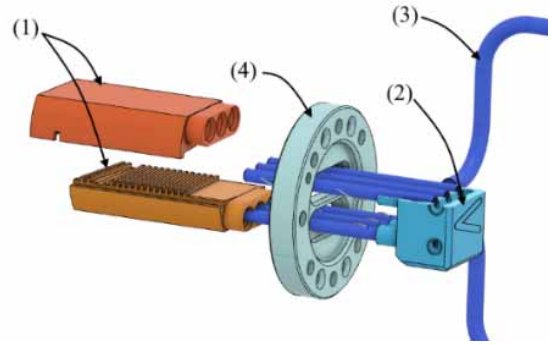

Figure 9: Main building blocks of the SLS2.0 absorber. (1) Milled upper and lower comb. The teeth and window geometries vary depending on the absorber type. (2) Cooling water distributor block made of Stainless Steel 316LN (3) Water cooling tubes with the spiral shaped channels made of Stainless Steel 316L. There are three cooling chambers per body, with collective inlet and outlet. (4) CF63 flange from 316LN Steel.

In the manufacturing process, all the parts are fixed together and brazed in one operation. After the manufacturing process, Quality Assurance tests are undertaken: vacuum leak test, hydrostatic leak test, magnetic permeability of the brazed joints as well as the geometrical check.

SUMMARY

SLS2.0 Storage ring will be equipped with more than twenty different absorbers that will sustain heat loads up to 7 kW. After the series of SR simulations, the geometries of the absorbers located downstream from the normal- and superbend dipoles and also undulators were proposed. After the validation of the maximal heat loads, finite element analysis was performed to validate the mechanical strength of the absorbers bodies. Subsequent CFD simulations showed the satisfactory results for the capacity of the water cooling. Prototype testing validated the simulation results for the heat load up to 6 kW. The final version of the absorbers is under manufacturing. The process of installation and alignment is under development.

ACKNOWLEDGEMENTS

The prototype's thermal test was performed with the support from Markus Maehr and Samuel Bugmann. The Authors of this paper would like to express the deep gratitude for their assistance.

ISBN: 978-3-95450-231-8 ISSN: 2673-5490 doi: 10.18429/JACoW-IPAC2023-THPA148

REFERENCES

[1] H.-H. Braun *et al.*, "SLS 2.0 storage ring. Technical design report", Paul Scherrer Institut, Villigen, Switzerland, Rep.21-02, 2021, https://www.dora.lib4ri.ch/psi/islandora/object/psi:39635

[2] R. Ganter *et al,.* "SLS2.0 vacuum components design", presented at IPAC'23, Venice, Italy, May 2023, paper THPA147, this conference.

[3] Molflow, https://molflow.web.cern.ch/.

[4] SPECTRA, https://spectrax.org/spectra/.

[5] F. Thomas *et al.*, "X-ray absorber design and calculations for the EBS storage ring", in *Proc. MEDSI'16*, Barcelona, Spain, Sep. 2016, pp. 257-261. doi:10.18429/JACoW-MEDSI2016-WEAA02

[6] M. Quispe, "Development of the Crotch absorbers for ALBA storage ring", in *Proc. MEDSI'08*, Jun. 2008, Saskatchewan, Canada.

[7] F. A. DePaola, C. Amundsen, and S. K. Sharma, "Manufacturing of photon beam-intercepting components from Cu-CrZr", in *Proc. MEDSI'16*, Barcelona, Spain, Sep. 2016, pp. 233-235. doi:10.18429/JACoW-MEDSI2016-TUPE31

[8] D. Lauper, "CHT Simulation eines Kühlkanals", CADFEM technical report CON-20-PAU-001_TB1, 2000

[9] FMB GmbH, https://www.fmb-berlin.de/index.php/de/.